Journal of

Mechanics of Materials and Structures

BRITTLE FRACTURE BEYOND THE STRESS INTENSITY FACTOR

C. T. Sun and Haiyang Qian

Volume 4, № 4 April 2009

mathematical sciences publishers

JOURNAL OF MECHANICS OF MATERIALS AND STRUCTURES
Vol. 4, No. 4, 2009

BRITTLE FRACTURE BEYOND THE STRESS INTENSITY FACTOR

C. T. SUN AND HAIYANG QIAN

It is commonly believed that the fracture toughness of a brittle material can be characterized by a single parameter such as the stress intensity factor. In this study, it was demonstrated that when the crack is highly constrained, the first nonsingular opening stress term at the crack tip, in addition to the K-field (the singular stress term), is necessary to predict fracture. Fracture experiments were conducted using plexiglass specimens with a center crack. Relatively rigid metallic end tabs were used to generate boundary constraints on the specimen. The level of constraint was varied by varying the gage length between the end tabs. For a given crack length, the fracture load increases as the gage length decreases. If the stress intensity factor is used to determine the corresponding fracture toughness of plexiglass, the experimental data would indicate that the fracture toughness decreases as the gage length decreases. This is equivalent to saying that the fracture toughness of a brittle material can be affected by boundary conditions. It was shown that this behavior is the result of a diminishing size of the K-dominance zone and that the stress intensity factor alone cannot fully capture the fracture force. A new constant parameter was introduced to account for the effect of the near-tip nonsingular stress field on fracture.

1. Introduction

It is a common notion that, for brittle materials, fracture can be characterized by a stress intensity factor alone and that the nonsingular part of the near-tip stress field may be ignored. However, it has been found in many situations that the use of stress intensity (or energy release rate) alone may lead to variable fracture toughness, resulting from constraining conditions on the crack. One of the notable examples is in adhesively bonded structural joints. Gardon [1963] performed an adhesive peeling test and found that the peeling force decreased as the adhesive layer became thinner. Bascom et al. [1975] and Bascom and Cottington [1976] discovered from the tapered double cantilever beam test that the strength of rubber-modified epoxy-bonded specimens increased with the decrease of the adhesive thickness. This behavior was subsequently confirmed by many researchers [Kin Loch and Shaw 1981; Daghyani et al. 1995a; 1995b; Ikeda et al. 2000; Yan et al. 2001; 2002; Lee et al. 2003; 2004] using the same adhesive material and similar specimens. Attempts were made to use plastic zone size and its shape ahead of the crack tip to qualitatively explain the adhesive thickness-dependent fracture toughness [Kin Loch and Shaw 1981].

Similar to adhesive joints, there are cracked elastic bodies in which the singular stress field (the K-field) is very small and may not be sufficient to describe the state of stress in the fracture process zone, and thus a constant stress intensity factor is not sufficient to characterize the fracture toughness of brittle materials. On the other hand, for elastic-plastic materials, Larsson and Carlson [1973] and Rice [1974] recognized the influence of T-stress (the first nonsingular normal stress parallel to the crack plane) on the

Keywords: stress intensity factor, K-dominance, fracture load, nonsingular stress, plexiglass.
This research was supported by a grant from the Federal Agency of Aviation for the JAMS Center of Excellence.

crack tip plastic zone size and on the fracture behavior. Since then, there have been numerous publications addressing different aspects of T-stress. For instance, Leevers and Radon [1982] introduced a biaxiality ratio to account for the effect of the nonsingular stress terms, and Kardomateas et al. [1993] used the biaxiality ratio to explain the difference between the fatigue crack growth rates of short cracks and long cracks.

The purpose of this research is to employ the concept of the K-dominance zone near the crack tip to gauge the importance of the nonsingular stress terms. We focus on relatively brittle materials so that the first nonsingular term in the near-tip opening stress, rather than the T-stress, is considered in characterizing the fracture condition. A center cracked plexiglass specimen clamped on both loading sides was used to conduct the fracture experiment. To vary the contribution of the nonsingular stress to the total opening stress near the crack tip, the distance between the clamps was varied. It is demonstrated that the near-tip stress field, especially the size of the region dominated by the singular stress field (the K-dominance zone), can be significantly altered by the boundary constraints resulting from the clamps. Consequently, the fracture load cannot be predicted using the stress intensity factor alone. A two-parameter fracture model is proposed to characterize a nonconstant apparent fracture toughness of plexiglass.

2. Specimens and fracture experiment

Center cracked plexiglass specimens as shown in Figure 1 were used in the fracture test. The thickness was 4.76 mm (0.1875 inch) for all specimens. The specimen width (W) was 76.2 mm (3 inch) and a crack of length ($2a$) 25.4 mm (1 inch) was created using a water jet cutting machine. The crack created in this manner was not sharp enough and was extended further for about a millimeter using a razor blade (see Figure 2). The height (T) of the end tabs was 38.1 mm (1.5 inch). Five different values of gage length ($2h$) were considered to vary the constraining effect of the boundary on the crack. The gage length was selected to yield six different ratios to the initial crack length: $h/a = 10$, 4, 2, 1, 0.5 and 0.25. The constraining effect on the crack is characterized by the h/a ratio.

Aluminum end tabs (3.9 mm thick) were bonded on the specimens. Fracture tests were performed on an MTS 22 kip machine under a constant displacement rate loading at 0.001 mm/sec.

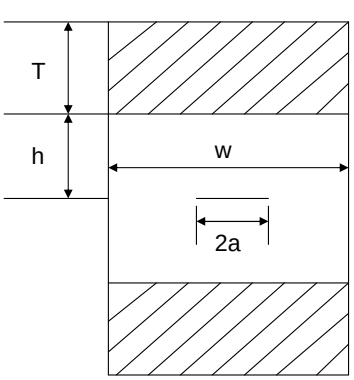

Figure 1. Specimen configuration.

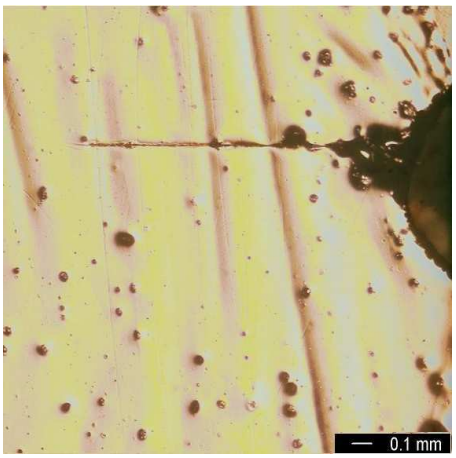

Figure 2. Sharp crack tip created by a razor blade.

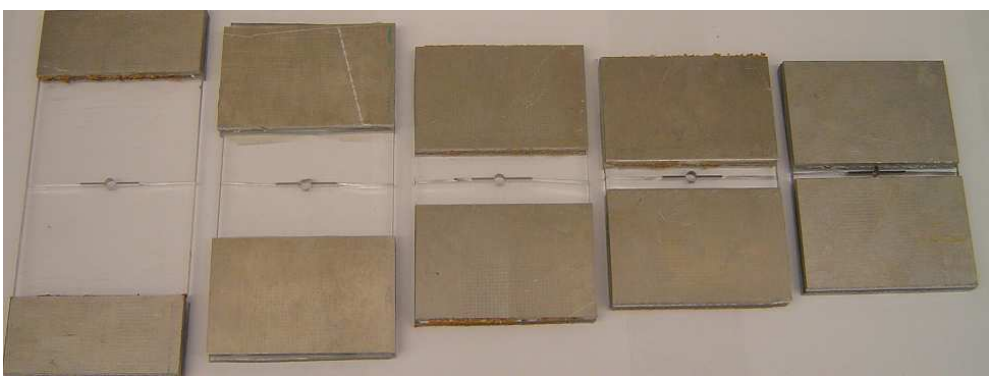

Figure 3. Specimens after fracture.

Figure 3 shows sample specimens with different gage lengths after the fracture test. The failure appears to be a typical brittle fracture failure and no stable crack growth was observed. For each gage length (h/a ratio), at least three specimens were tested. Figure 4 shows the failure loads for specimens with the six gage lengths. The data clearly show that for h/a smaller than 2, the average strength of the specimens increases with decreasing h/a value. For h/a ratios larger than 2, the failure load appears to approach a constant. In other words, the strength of the specimen is not affected by the gage length when the constraining effect diminishes. On the other hand, the strength of the specimen seems to keep increasing as the gage length decreases.

3. Analysis of fracture data

3.1. ***Finite element model.*** The elastic stress analysis is performed using the commercial finite element code ABAQUS 6.6. In view of the symmetric configuration of the specimen, a quadrant of the specimen is modeled. Symmetric boundary conditions are applied along the corresponding edges of symmetry. Because aluminum has a much greater elastic modulus than plexiglass, the clamped boundary can be

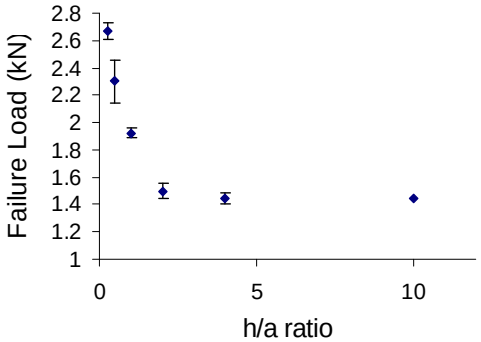

Figure 4. Experimental failure loads for different h/a ratios.

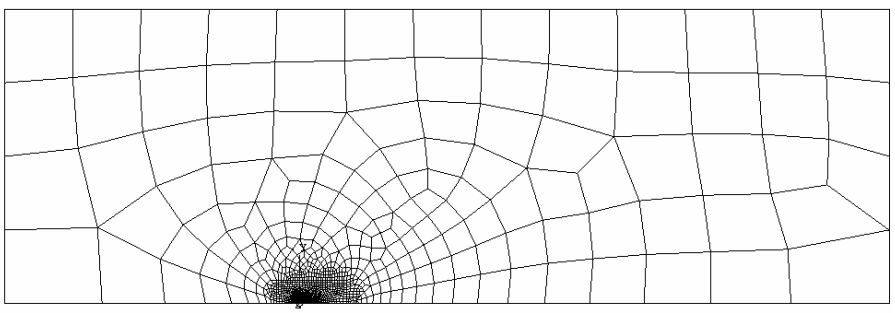

Figure 5. Finite element mesh for specimen with $h/a = 1$.

regarded as a rigid boundary so that a uniform displacement loading is assumed. In the numerical analysis, the crack length is the initial crack length created by the water jet plus the small extension produced by the razor blade.

Figure 5 shows the typical configuration and mesh of one of the models for $h/a = 1$. A 4-node plane strain element (CPE4) is used. In order to capture the high stress gradient field near the crack tip for small gage length cases, relatively fine mesh sizes are adopted around the crack tip. The smallest element size is less than 0.0001 of the half crack length which ensures converged solutions. The mesh around the crack tip is also made uniform in order to facilitate the computation of the energy release rate using the modified crack closure method [Rybicki and Kanninen 1977]. The stress intensity factor is then obtained from its relation with the energy release rate. An elastic Young's modulus for the plexiglass of 2.8 GPa (reported by the manufacturer) and a Poisson's ratio of 0.3 are used in the calculation.

3.2. ***Conventional LEFM fracture prediction.*** In linear elastic fracture mechanics (LEFM), the stress intensity factor is used to characterize the fracture toughness (K_c) of a brittle material. For a given specimen thickness the value of K_c is assumed to be a constant. To check the validity of the this assumption regarding the specimen configuration, the stress intensity factors for different h/a ratios are calculated for an applied load of 2 kN, with the result given in Figure 6. It is seen that the stress intensity factor is greatly influenced by the h/a ratio in the range of h/a smaller than 4. In LEFM, fracture toughness is considered as a material constant and is used as the single parameter to predict fracture failure. If this assumption is valid, then the value of K_c can be determined using the specimen with $h/a = 4$ and then

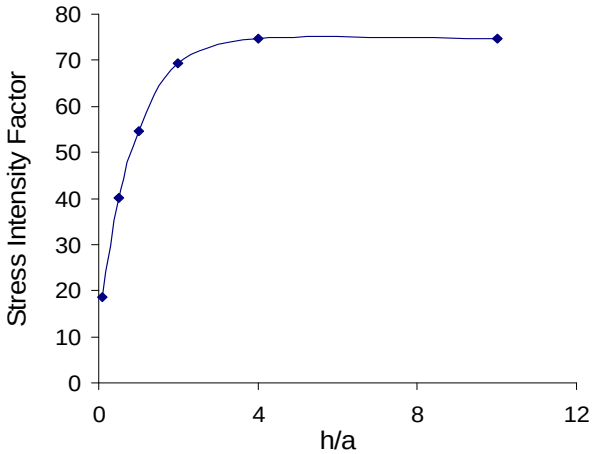

Figure 6. Effect of h/a ratio on stress intensity factor.

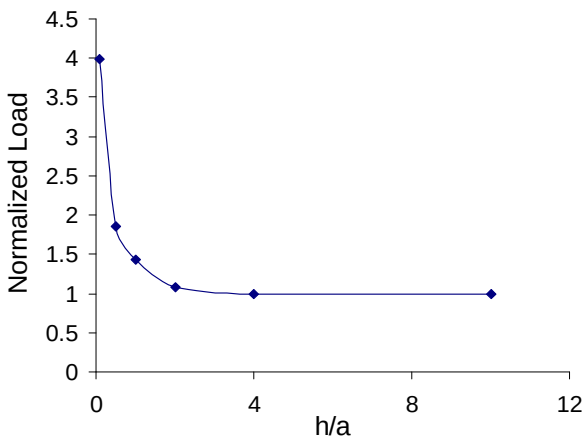

Figure 7. Failure loads (for the same critical stress intensity factor) normalized by the failure load corresponding to $h/a = 4$.

used to predict the failure loads for other specimens with smaller h/a ratios, as shown in Figure 7. (All failure loads in that figure are normalized with respect to the failure load for $h/a = 4$.)

3.3. ***Comparison with experimental result.*** From the results presented in Figures 6 and 7, the fracture toughness approaches a constant value K_c^∞ for $h/a \geq 4$. If this K_c^∞ value is used to predict the failure loads for all specimens with different h/a ratios, then the predicted failure loads for h/a smaller than 4 deviate significantly from the experimental results, as shown in Figure 8. Note that in Figure 8, the experimental failure load is normalized with respect to the failure load of the specimen with $h/a = 4$. It is evident that the LEFM prediction appears to be valid only for h/a ratios larger than 4, for which the boundary constraining effect diminishes and the stress intensity factor is a constant value for a given applied load (see Figure 6). If a single K_c parameter is to be adopted to characterize the fracture toughness of plexiglass, then the value of K_c must be a function of h/a (see Figure 9). The asymptotic value K_c^∞ as the fracture toughness is only valid for large values of h/a ratios.

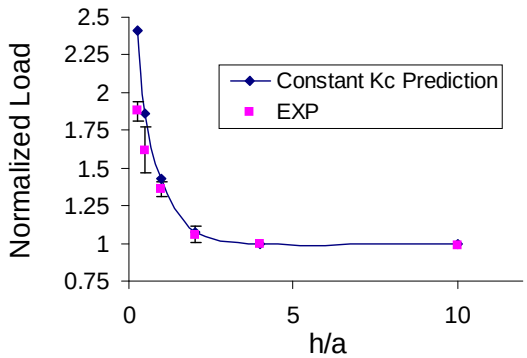

Figure 8. Comparison of LEFM prediction and experimental data.

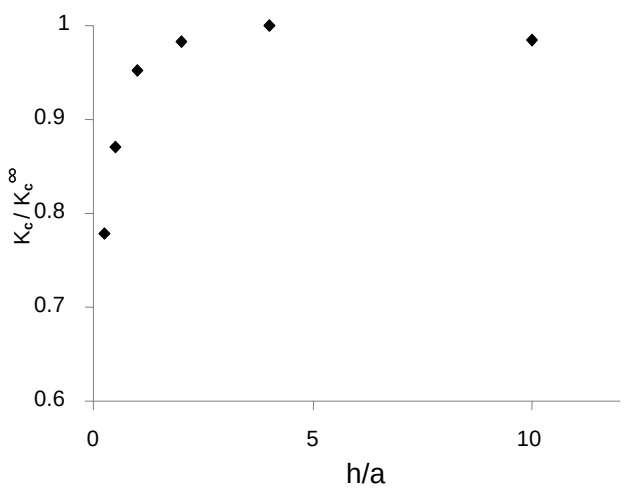

Figure 9. Apparent K_c based on LEFM and experimental failure load.

4. *K*-dominance zone analysis

The reason that a single parameter K_c is sufficient to characterize fracture toughness in brittle materials is based on the assumption that the singular stress field (the K field) is the dominant stress field near the crack tip and that the "fracture process" zone is totally contained inside the K-dominance zone. If this assumption is not valid then the fracture process may be influenced by the nonsingular part of the near tip stress. Thus, to explain the discrepancy displayed in Figure 8, the size of the K-dominance zone must be investigated.

The total opening stress ahead of the crack tip can be expressed in a general form as

$$\sigma_{yy} = \frac{K}{\sqrt{2\pi x}} + \text{ nonsingular stress}, \tag{1}$$

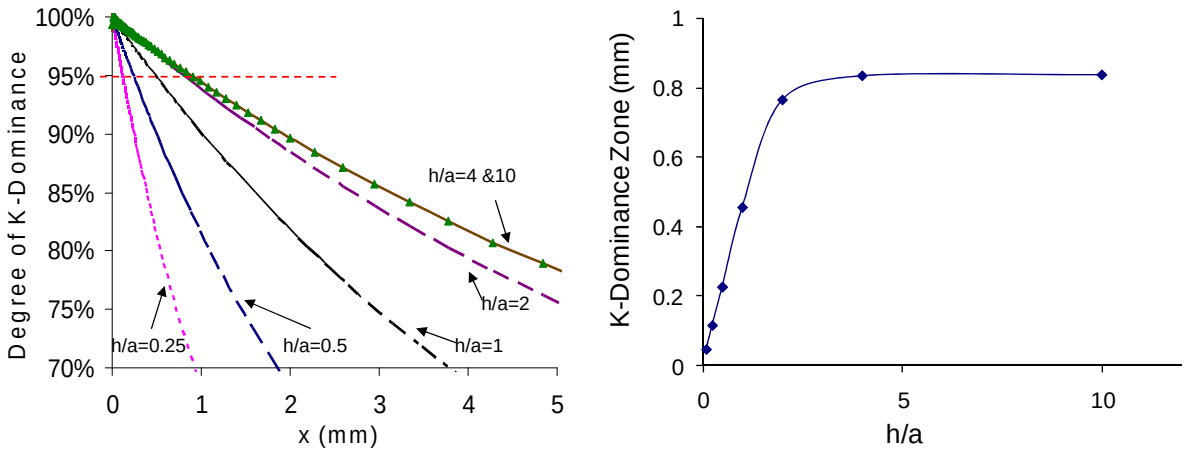

Figure 10. Left: K-dominance as a function of x. Right: Size of the K-dominance zone (region where $\Lambda \geq 95\%$).

where K is the stress intensity factor and x is the distance from the crack tip. At a given location x, the weight of the singular term can be quantified by the degree of K-dominance defined as

$$\Lambda = \frac{\sigma_{yy}^{\text{Singular}}}{\sigma_{yy}^{\text{Singular}} + \left|\sigma_{yy}^{\text{Nonsingular}}\right|}, \tag{2}$$

where

$$\sigma_{yy}^{\text{Singular}} = \frac{K}{\sqrt{2\pi x}}, \quad \sigma_{yy}^{\text{Nonsingular}} = \sigma_{yy} - \sigma_{yy}^{\text{Singular}}.$$

The value of Λ represents the percentage of the singular stress in the total opening stress at a given location. Figure 10, left, shows the degree of K-dominance as a function of the distance from the crack tip. As expected, for all the curves, the value of Λ starts from 100% at the crack tip and then decreases as the distance from the crack tip increases. Note that Λ drops much faster in specimens with smaller gage lengths (h/a ratio) than those with larger gage lengths; for h/a ratios larger than 4, the Λ curves approach a limiting curve.

Define the K-dominance zone as the region in which $\Lambda \geq 95\%$; this region can be determined from the plot of Λ, and its dependence on h/a is shown in Figure 10, right. Clearly, the size of the K-dominance zone becomes a constant for $h/a \geq 4$. Below this ratio, the zone shrinks significantly as the h/a ratio decreases.

We conclude from these results that, as the gage length (or h/a) decreases, the nonsingular stress may not be negligible compared to the singular term in the near-tip region. In other words, the stress intensity factor cannot fully represent the stress field except for a region extremely close to the crack tip. This is why the stress intensity factor alone cannot adequately serve as the fracture failure criterion.

5. Two-parameter model

As we saw in Figure 10, the K-dominance zone decreases as the h/a ratio decreases. This indicates that the stress intensity factor is no longer sufficient to represent the full stress effect ahead of the crack tip

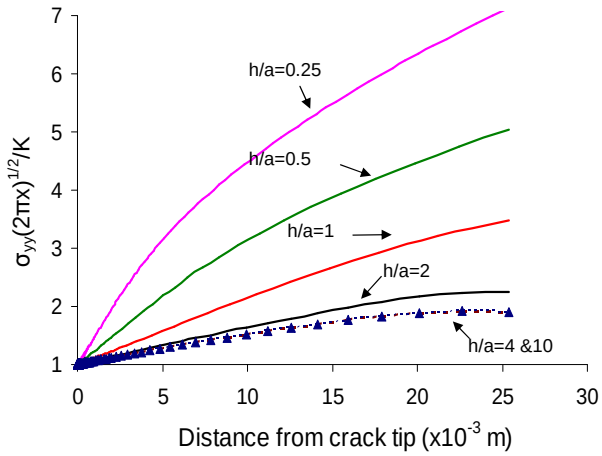

Figure 11. Distribution of opening stress ahead of the crack tip.

and that the nonsingular stress may be needed to predict the fracture load. From William's expansion of the near-tip opening stress we have

$$\sigma_{yy}\sqrt{2\pi x} = K + C_0\sqrt{2\pi}\,x + C_1\sqrt{2\pi}\,x^{3/2} + \cdots . \tag{3}$$

The $\sigma_{yy}\sqrt{2\pi x}$ vs. x curves for various h/a ratios are calculated and plotted in Figure 11. Note that in Figure 11, loads are selected so that the same stress intensity factor is produced for all cases of h/a ratios. As shown in Figure 11, the magnitude of the nonsingular stress may become comparable to the singular stress at a small distance from the crack tip, especially for those associated with smaller h/a ratios. It is also found that the near tip opening stress distributions for $h/a = 4$ and $h/a = 10$ are almost identical. This shows that the boundary constraining effect vanishes when the h/a ratio reaches a certain value ($h/a = 4$ in this case).

It is seen from Figure 11 that $\sigma_{yy}\sqrt{2\pi x}$ increases almost linearly with respect to x near the crack tip and can be closely approximated as

$$\sigma_{yy}\sqrt{2\pi x} = K + Ax. \tag{4}$$

Rearranging (4), we have

$$\sigma_{yy}\sqrt{2\pi x}/K = 1 + Cx \quad (C = A/K). \tag{5}$$

The value of the coefficient C depends on the value of h/a and can be obtained from the result of Figure 11:

$$C = \big(65(h/a)^{-1.3} + 61.37\big)\mathrm{m}^{-1}. \tag{6}$$

Note that the value of C approaches a constant $C_0 = 61.37\mathrm{m}^{-1}$ as h/a increases beyond 4.

Define the effective stress intensity factor based on the expression of (4) as

$$K^{\mathrm{eff}} = \sigma_{yy}\sqrt{2\pi x_0} = K + Ax_0, \tag{7}$$

where x_0 is a critical distance to be determined from the experimental result. If, in addition, we set

$K^{\text{eff}} = K_c^{\infty}$ for $h/a \geq 4$, then (7) becomes

$$K_c^{\infty} = K_c + Ax_0 = K_c(1 + Mx_0), \tag{8}$$

where

$$M = C - 61.37 = 65(h/a)^{-1.3}\text{m}^{-1}. \tag{9}$$

From (8), the apparent fracture toughness for any given h/a ratio is given by

$$K_c = K_c^{\infty}/(1 + Mx_0). \tag{10}$$

Finally, the critical distance x_0 is determined by least square fitting of the experimental data for six different h/a ratios, shown in Figure 9. We obtain $x_0 = 0.75$ mm. Thus the apparent fracture toughness K_c can be explicitly expressed as

$$K_c = \frac{K_c^{\infty}}{1 + Mx_0} = \frac{K_c^{\infty}}{1 + 0.49(h/a)^{-1.3}}. \tag{11}$$

The above equation indicates that the decrease of the K-dominance zone size with the h/a ratio reduces the apparent fracture toughness. Figure 12 shows the experimental K_c together with the result obtained from (11).

To predict the failure load for a given h/a ratio, the apparent fracture toughness K_c calculated according to (11) is used. In (11), effective fracture toughness K^{eff} and critical distance x_0 are regarded as material constants and coefficient A is obtained from the near-tip opening stress calculated by the FEA. Figure 13 shows the comparison of the failure loads obtained using the constant $K_c = K_c^{\infty}$ and the two-parameter model, respectively. It can be seen that the two parameter model is more adequate in predicting the failure load. It is of interest to note that the two-parameter model predicts that the failure load would begin to decrease rapidly at the h/a ratio around 0.1. In fact, based on (11), the failure load would diminish as the h/a ratio approaches zero. The validity of this result needs further experimental verification.

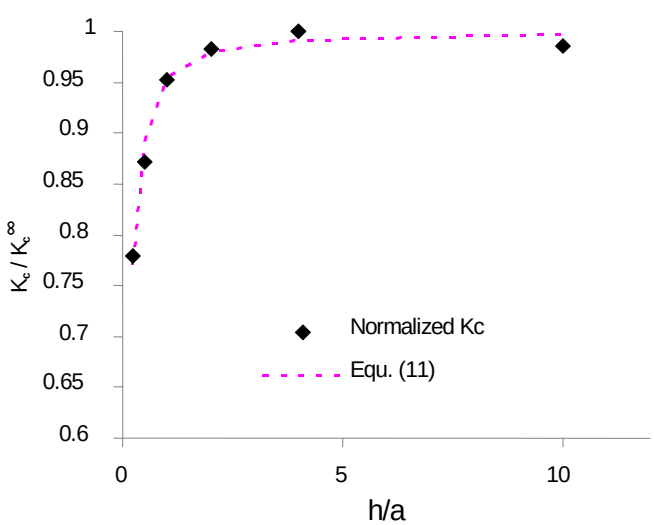

Figure 12. Apparent fracture toughness K_c predicted by Equation (11).

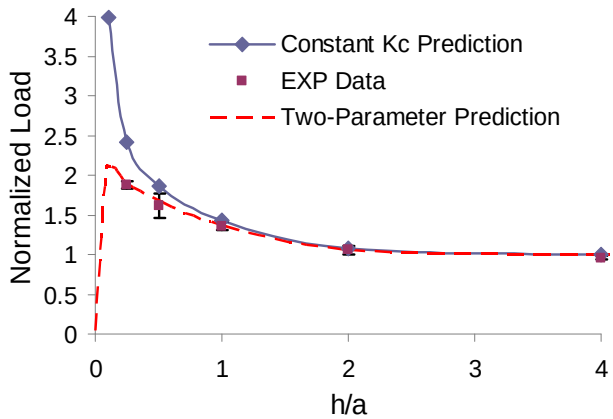

Figure 13. Failure load according to the two-parameter model.

6. Conclusion

It has been demonstrated that even for materials commonly considered as brittle, the LEFM may not always be adequate for characterizing their toughness properties. The main reason lies in the fact that, under some boundary conditions, the crack tip region in which the singular stress represented by the stress intensity factor (the K-field) becomes very small and cannot adequately describe the fracture force. Consequently, the nonsingular part of the opening stress field in addition to the K-field is needed to predict fracture. The two-parameter model that includes the stress intensity factor and the first dominant nonsingular stress term seems to be capable of predicting fracture loads for plexiglass under general crack tip stress conditions.

Acknowledgement

During the sixties at Northwestern University, Professor George Herrmann built a group of outstanding mechanics faculty who went on to gain prominence in the international mechanics community. Sun was fortunate to be a graduate student with him at that time.

References

[Bascom and Cottington 1976] W. D. Bascom and R. L. Cottington, "Effect of temperature on the adhesive fracture behavior of an elastomer-epoxy resin", *J. Adhesion* **7**:4 (1976), 333–346.

[Bascom et al. 1975] W. D. Bascom, R. L. Cottington, R. L. Jones, and P. Peyser, "The fracture of epoxy- and elastomer-modified epoxy polymers in bulk and as adhesives", *J. Appl. Polym. Sci.* **19**:9 (1975), 2545–2562.

[Daghyani et al. 1995a] H. R. Daghyani, L. Ye, and Y. W. Mai, "Mode-I fracture behaviour of adhesive joints, I: Relationship between fracture energy and bond thickness", *J. Adhesion* **53**:3–4 (1995), 149–162.

[Daghyani et al. 1995b] H. R. Daghyani, L. Ye, and Y. W. Mai, "Mode-I fracture behaviour of adhesive joints, II: Stress analysis and constraint parameters", *J. Adhesion* **53**:3–4 (1995), 163–172.

[Gardon 1963] J. L. Gardon, "Peel adhesion, I: Some phenomenological aspects of the test", *J. Appl. Polym. Sci.* **7**:2 (1963), 625–641.

[Ikeda et al. 2000] T. Ikeda, A. Yamashita, D. Lee, and N. Miyazaki, "Failure of a ductile adhesive layer constrained by hard adherends", *J. Eng. Mater. Technol.* (*ASME*) **122**:1 (2000), 80–85.

[Kardomateas et al. 1993] G. A. Kardomateas, R. L. Carlson, A. H. Soediono, and D. P. Schrage, "Near tip stress and strain fields for short elastic cracks", *Int. J. Fract.* **62**:3 (1993), 219–232.

[Kin Loch and Shaw 1981] A. J. Kin Loch and S. J. Shaw, "The fracture resistance of a toughened epoxy adhesive", *J. Adhesion* **12**:1 (1981), 59–77.

[Larsson and Carlson 1973] S. G. Larsson and A. J. Carlson, "Influence of non-singular stress terms and specimen geometry on small-scale yielding at crack tips in elastic-plastic materials", *J. Mech. Phys. Solids* **21**:4 (1973), 263–277.

[Lee et al. 2003] D. B. Lee, T. Ikeda, N. Miyazaki, and N. Choi, "Fracture behavior around a crack tip in rubber-modified epoxy adhesive joint with various bond thicknesses", *J. Mater. Sci. Lett.* **22**:3 (2003), 229–233.

[Lee et al. 2004] D. B. Lee, T. Ikeda, N. Miyazaki, and N. Choi, "Effect of bond thickness on the fracture toughness of adhesive joints", *J. Eng. Mater. Technol.* (*ASME*) **126**:1 (2004), 14–18.

[Leevers and Radon 1982] P. S. Leevers and J. C. Radon, "Inherent stress biaxiality in various fracture specimen geomtries", *Int. J. Fract.* **19**:4 (1982), 311–325.

[Rice 1974] J. R. Rice, "Limitations to the small scale yielding approximation for crack tip plasticity", *J. Mech. Phys. Solids* **22**:1 (1974), 17–26.

[Rybicki and Kanninen 1977] E. F. Rybicki and M. F. Kanninen, "A finite element calculation of stress intensity factors by a modified crack closure integral", *Eng. Fract. Mech.* **9**:4 (1977), 931–938.

[Yan et al. 2001] C. Yan, Y. W. Mai, Q. Yuan, L. Ye, and J. Sun, "Effects of substrate materials on fracture toughness measurement in adhesive joints", *Int. J. Mech. Sci.* **43**:9 (2001), 2091–2102.

[Yan et al. 2002] C. Yan, K. Xiao, L. Ye, and Y. W. Mai, "Numerical and experimental studies on the fracture behavior of rubber-toughened epoxy in bulk specimen and laminated composites", *J. Mater. Sci.* **37**:5 (2002), 921–927.

Received 10 Mar 2008. Revised 7 Oct 2008. Accepted 6 Dec 2008.

C. T. SUN: sun@purdue.edu
Purdue University, School of Aeronautics and Astronautics, 701 W. Stadium Ave, W. Lafayette, IN 47907, United States

HAIYANG QIAN: hqian@purdue.edu
Purdue University, School of Aeronautics and Astronautics, 701 W. Stadium Ave, W. Lafayette, IN 47907, United States